



Journal of Enzyme Inhibition and Medicinal Chemistry

ISSN: 1475-6366 (Print) 1475-6374 (Online) Journal homepage: <https://www.tandfonline.com/loi/ienz20>


Antiproliferative and antibacterial activity of some glutarimide derivatives

Jelena B. Popović-Djordjević, Anita S. Klaus, Željko S. Žižak, Ivana Z. Matic & Branko J. Drakulić


To cite this article: Jelena B. Popović-Djordjević, Anita S. Klaus, Željko S. Žižak, Ivana Z. Matic & Branko J. Drakulić (2016) Antiproliferative and antibacterial activity of some glutarimide derivatives, *Journal of Enzyme Inhibition and Medicinal Chemistry*, 31:6, 915-923, DOI: [10.3109/14756366.2015.1070844](https://doi.org/10.3109/14756366.2015.1070844)

To link to this article: <https://doi.org/10.3109/14756366.2015.1070844>


 View supplementary material 

 Published online: 06 Aug 2015.

 Submit your article to this journal 

 Article views: 525

 View Crossmark data 

 Citing articles: 3 View citing articles 

RESEARCH ARTICLE

Antiproliferative and antibacterial activity of some glutarimide derivatives

Jelena B. Popović-Djordjević¹, Anita S. Klaus², Željko S. Žižak³, Ivana Z. Matic³, and Branko J. Drakulić⁴

¹Department of Chemistry and Biochemistry and ²Department for Industrial Microbiology, Faculty of Agriculture, University of Belgrade, Belgrade, Serbia, ³Institute of Oncology and Radiology of Serbia, Belgrade, Serbia, and ⁴Department of Chemistry, Institute of Chemistry, Technology and Metallurgy, University of Belgrade, Belgrade, Serbia

Abstract

Antiproliferative and antibacterial activities of nine glutarimide derivatives (**1–9**) were reported. Cytotoxicity of compounds was tested toward three human cancer cell lines, HeLa, K562 and MDA-MB-453 by MTT assay. Compound **7** (2-benzyl-2-azaspiro[5.11]heptadecane-1,3,7-trione), containing 12-membered ketone ring, was found to be the most potent toward all tested cell lines (IC₅₀ = 9–27 μM). Preliminary screening of antibacterial activity by a disk diffusion method showed that Gram-positive bacteria were more susceptible to the tested compounds than Gram-negative bacteria. Minimum inhibitory concentration (MIC) determined by a broth microdilution method confirmed that compounds **1**, **2**, **4**, **6–8** and **9** inhibited the growth of all tested Gram-positive and some of the Gram-negative bacteria. The best antibacterial potential was achieved with compound **9** (ethyl 4-(1-benzyl-2,6-dioxopiperidin-3-yl)butanoate) against *Bacillus cereus* (MIC 0.625 mg/mL; 1.97×10^{-3} mol/L). Distinction between more and less active/inactive compounds was assessed from the pharmacophoric patterns obtained by molecular interaction fields.

Introduction

Both naturally occurring and synthetic cyclic imides, especially five- and six-membered systems, are an important group of bioactive molecules. They exhibit widespread pharmacological effects, including antitumor^{1–4}, anti-inflammatory⁵, immunomodulatory, antiangiogenic and anxiolytic^{6–8}.

Isolation and examination of pharmacologically active natural glutarimides started in 1960s. Initially, cycloheximide⁹ and streptimidone^{10–12} were examined as antibiotics, but later it was found that they acted as very potent cytotoxic agents^{13,14}. The structurally related streptimidone derivative, 9-methylstreptimidone, exerts a significant inhibitory activity toward nuclear factor-κB (N-κB)¹⁵. N-κB is involved in cancer and inflammations. Alkaloids (+)-sesbanimide A and (–)-sesbanimide B were isolated from the seeds of the leguminous plant *Sesbania drummondii*^{1,16}. Ethanol extracts of *S. drummondii* seeds showed significant inhibitory activity against P388 murine leukemia model in mice (*in vivo*)^{17–19}. Structurally related natural product lactimidomycin (LTM), 12-membered unsaturated macrolide antibiotic that comprise biosynthetically rare glutarimide side chain, produced by *Streptomyces amphibiosporus* R310-104 (ATCC 53964), display strong cytotoxicity against a number of human tumor cell lines *in vitro*, *in vivo* antitumor activity in mice model and potent antifungal activity².

Keywords

Antitumor agents, heterocycles, structure–activity analysis

History

Received 7 May 2015
Revised 25 June 2015
Accepted 26 June 2015
Published online 6 August 2015

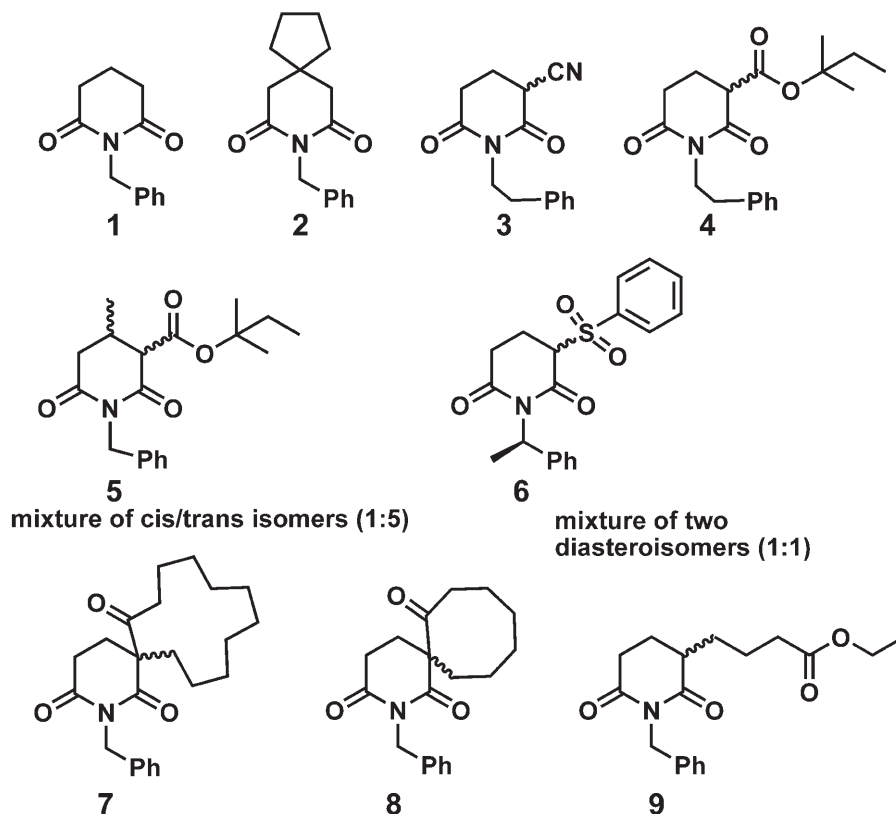
In 1990s it was discovered that thalidomide, a well-known synthetic glutarimide derivative, has anti-inflammatory and antiangiogenic properties. It was approved as a drug for the treatment of certain cancers (newly diagnosed multiple myeloma) and for complication arisen from leprosy. Later on, analogs of thalidomide with increased potency, 3-amino-thalidomid (pomalidomid, Pomalyst) and α-(3-aminophthalimido) glutarimide (lenalidomid, Revlimid) have been developed^{20,21}. Lenalidomid has been used for the treatment of multiple myeloma, while pomalidomid has been recently approved by FDA for the treatment of relapsed and refractory multiple myeloma²².

Some estrone derivatives with the D-ring replaced with the glutarimide moiety showed potent inhibition of steroid sulfatase, an enzyme involved in the pathway of the development of hormone-dependent breast tumors²³; while aminoglutethimide, the non-steroidal aromatase inhibitor, is in use for the treatment of hormone-sensitive metastatic breast cancer^{24,25}. In the past decade, antitumor activity *in vitro* of mitonafide²⁶, amonafide²⁷ and naphthalimide^{28,29} derivatives was intensively examined.

Upon detail analysis of bioactive compounds that comprise glutarimide moiety in their structure, as is briefly outlined in previous paragraphs, we concluded that data on antiproliferative and on antibacterial activity of compounds **1–9** (Figure 1) cannot be found in literature. Those compounds have been prepared in our group to demonstrate novel synthetic approach of glutarimide ring closure reaction³⁰. All compounds have a common *N*-substituted glutarimide moiety in their structure, and bear structurally diverse substituents in positions 3 and/or 4 of glutarimide ring. We have tested antiproliferative and antibacterial activity of compounds **1–9** *in vitro*, and hereby report on the results obtained.

Address for correspondence: Jelena B. Popović-Djordjević, Department of Chemistry and Biochemistry, Faculty of Agriculture, University of Belgrade, Nemanjina 6, 11080 Belgrade, Serbia. E-mail: jelenadj@agrif.bg.ac.rs

Figure 1. Structures of glutarimide derivatives 1–9.



Methods

Antiproliferative activity

Stock solutions of investigated compounds were prepared in a nutrient medium (RPMI-1640) supplemented with 3 mM L-glutamine, 100 µg/mL streptomycin, 100 IU/mL penicillin, 10% heat inactivated fetal bovine serum (FBS) and 25 mM HEPES, adjusted to pH 7.2 by bicarbonate solution. RPMI-1640, FBS, HEPES and L-glutamine were products of Sigma Chemical Co., St. Louis, MO. Human cervix adenocarcinoma HeLa, breast carcinoma MDA-MB-453 and normal lung fibroblast MRC-5 cells were cultured as monolayers in the nutrient medium, while human myelogenous leukemia K562 cells were maintained as suspension culture. The cells were grown at 37 °C in 5% CO₂ and humidified air atmosphere.

HeLa (2000 cells per well), MDA-MB-453 (3000 c/w) and MRC-5 (5000 c/w) cells were seeded into 96-well microtiter plates and 20 h later, after the cell adherence, five different concentrations of investigated compounds were added to the wells. Final concentrations were in the range from 200 to 12.5 µM. Only nutrient medium was added to the cells in the control wells. Investigated compound was added to a suspension of leukemia K562 cells (5000 cells/well) 2 h after cell seeding, in the same final concentrations applied to HeLa, MDA-MB-453 and MRC-5 cells. All experiments were done in triplicate. Nutrient medium with corresponding concentrations of compound, but void of cells, was used as blank.

Cell survival was determined by MTT test according to the method of Mosmann and modified by Ohno and Abe, 72 h after addition of the compounds^{31,32}. Briefly, 20 µL of MTT solution (5 mg/mL in phosphate buffered saline) was added to each well. Samples were incubated for further 4 h at 37 °C in humidified atmosphere with 5% CO₂. Then, 100 µL of 10% SDS was added to

the wells. Absorbance was measured at 570 nm the next day. To achieve cell survival (S%), absorbance at 570 nm of a sample with cells grown in the presence of various concentrations of compounds tested was divided with absorbance of control sample (the absorbance of cells grown in nutrient medium only). Absorbance of blank was always subtracted from absorbance of a corresponding sample with cells. All experimentally obtained IC₅₀ data were means of three measurements done in triplicate.

The antibacterial activity testing

The antibacterial activity of compounds 1, 2, 4–8 and 9 was determined against four Gram-positive (*Staphylococcus aureus*, *Enterococcus faecalis*, *Bacillus cereus*, *Listeria monocytogenes*) and seven Gram-negative bacterial species [*Pseudomonas aeruginosa*, *Escherichia coli*, *Salmonella enteritidis*, *Proteus hauseri*, *Shigella sonnei*, *Yersinia enterocolitica*, *E. coli* (O157:H7)]. Selected bacterial strains originated from ATCC (American Type Culture Collection, Rockville, MD). These microorganisms were chosen for the bioassay as the well-known food spoilage and pathogenic bacteria. Each species was maintained on Mueller–Hinton agar (MHA), which was also used to confirm the absence of contamination and the validity of the inocula. Before testing, each species was recovered by sub-culturing in Mueller–Hinton broth (MHB), aerobically, for 24 h, at 37 °C. Working concentrations of approximately 10⁵–10⁶ cfu/mL, used for antibacterial activity assays, were prepared by proper dilution of culture in microbiological medium. Compounds were dissolved in DMSO (2%) to prepare stock solutions at a concentration of 40 mg/mL, sterilized by filtration through a 0.22-µm membrane filter (Sartorius AG – Göttingen, Germany) according to Tepe et al. and further diluted in MHB to a working solutions. DMSO was chosen as a non-toxic solvent³³.

Disk diffusion assay was performed using a slightly modified CLSI³⁴. Each bacterial culture (approximately 10^5 – 10^6 cfu/mL) was added (0.1 mL) to Petri dishes (90 mm) containing MHA (20 mL). Three sterile blank paper disks (6 mm in diameter, Susceptibility Test Discs, SD 067-5CT, HiMedia, Mumbai, India) were placed on the surface of each agar plate and inoculated with 10 μ L of the compound (20 mg/mL). After 2 h at 25 °C, the plates were incubated aerobically, for 24 h at 37 °C. After incubation period, inhibition zone (mm) was measured including the initial diameter of the disk. Tests were performed in triplicate and the results were analyzed for statistical significance. The plates with MHA were sterility controls. Negative controls were disks impregnated with DMSO. As positive controls disks (Sigma-Aldrich GmbH, Steinheim, Germany) with gentamicin (30 μ g) and tetracycline (30 μ g) were used.

Broth microdilution method was employed to determine minimum inhibitory concentrations (MICs)^{34,35}. Concentrations of compound ranged from 10.0 to 0.048 mg/mL. Test bacterial culture (50 μ L) in a MHB was added to the wells of a sterile 96-well microtiter plate (Sarstedt, Numbrecht, Germany) already containing 50 μ L of twofold serially diluted compound in MHB. The final volume in each well was 100 μ L. The microplates were prepared in triplicate and incubated aerobically, for 24 h at 37 °C. Wells with MHB was used as a sterility control, while negative controls were wells with tested compound in 50 μ L of MHB, but void of bacteria. Positive controls were wells with a bacterial suspension in 50 μ L of MHB and wells with a bacterial suspension in a MHB with DMSO, in amounts corresponding to the highest quantity present in the broth microdilution assay (to prove that DMSO had no inhibition effect on the bacterial growth). A microplate shaker (Lab Companion, VM-96B, Seoul, South Korea) was used for mixing the content of each well at 900 rpm for 1 min prior to incubation in the cultivation conditions described above. To indicate cellular respiration 2,3,5-triphenyltetrazolium chloride (TTC) (Aldrich Chemical Company Inc., Sigma-Aldrich, St. Louis, MO) was added to the culture medium. The final concentration of TTC after inoculation was 0.05%. Viable microorganisms enzymatically reduced white TTC to a pink TPF (1,3,5-triphenylformazan). The MIC was defined as the lowest sample concentration that prevented this change and exhibited complete inhibition of bacterial growth.

All measurements were done in triplicate and data were expressed as mean \pm standard deviation. The experimental data were subjected to an one-way analysis of variance (ANOVA) and Fisher's LSD was calculated to detect significant difference ($p \leq 0.05$) between the mean values.

Molecular modeling

Initial 3D structures of compounds **1**–**9** were generated from SMILES notation in CORINA assuming *R* stereochemistry for all stereogenic centers, except for C2 of the phenethyl moiety of compound **6**^{36,37}. The *S* stereochemistry was ascribed to this stereogenic center, on the ground of experimental data³⁰. Initial structures were imported in VegaZZ³⁸. Up to 20 conformations, representing local energy minima, were obtained by conformational search on the molecular mechanics level (MMFF94s force field), using Boltzmann jump algorithm in AMMP^{39,40}. Each conformation of each compound was minimized by the semi-empirical molecular orbital PM6 method, using implicit solvation in water (COSMO) to root mean square gradient of 0.01; by MOPAC2012^{41,42}. Conformation of each compound that had the lowest heat of formation (implying the most stable one) was chosen for further modeling. 3D-dependent whole-molecular properties of compounds, surface area, polar surface area, apolar

surface area, volume and virtual log *P*, were calculated in VegaZZ, using 1.4 Å probe⁴³. Molecular interaction fields (MIF) around molecules were calculated by a GRID method, as applied in Pentacle program, using grid resolution of 0.4 Å⁴⁴. Hydrogen-bond donor (N1), hydrogen-bond acceptor (O), hydrophobic (DRY) and shape (TIP) probes were used. AMANDA algorithm were used for the extraction of hot spots (nodes) from the obtained MIFs (discretization); the distances and relative position of the nodes were described by maximum auto- and cross-correlation (MACC2) (encoding). For more exhaustive description of applied methodology see original reference⁴⁵. Auto- and cross-correlograms, obtained by the Pentacle program are depicted in matrix-like representation, named as heatmap. Values of variables are color-coded from red (low value) to blue (high value). For color code in heatmap, depicted in Figure 3, see on-line version of the article. Correlograms encode molecular descriptors grounded on two-point pharmacophoric pattern, which represent the local minima of two probes (nodes) around molecule, including distance between those nodes. All blocks of correlograms (DRY-DRY, O-O, N1-N1, TIP-TIP, DRY-O, DRY-N1, DRY-TIP, O-N1, O-TIP, N1-TIP) were considered during analysis.

Chemistry

Chemicals and solvents were purchased from Merck (Darmstadt, Germany), Sigma-Aldrich and Fluka (Basel, Switzerland). All reagents were of analytically pure. All solvents were dried by standard methods and distilled before use. The sodium hydride was used as a 60% dispersion in mineral oil. 18-Crown-6 ether was prepared according to a literature procedure⁴⁶. Reactions were monitored on silica gel pre-coated TLC plates, HF₂₅₄ (Merck). The dry-flash chromatography on silica gel (12–16 μ , ICN Pharmaceuticals, Costa Mesa, CA) was used to purify the reaction products. Anhydrous reactions were carried out in oven-dried glassware in extra pure argon atmosphere. ¹H and ¹³C NMR spectra were recorded on a Bruker Avance 500 (Bruker BioSpin GmbH, Karlsruhe, Germany), or Varian (Palo Alto, CA) Gemini 2000 instruments on 500/125 or 200/50 MHz, in CDCl₃ with TMS as an internal reference. ESI-MS spectra were recorded on Agilent Technologies (Santa Clara, CA) 6210-1210 TOF-LC-ESI-HR/MS instrument in positive mode. Integrity and purity of all compounds used for biological tests are routinely checked by NMR and ESI/HR-MS.

General procedure for the synthesis of compounds **1** and **2**

1-Benzyl-piperidine-2,6-dione (**1**, C₁₂H₁₃NO₂). Toluene (20 mL) and sodium hydride (2.9 g, 72 mmol) were placed in a two-necked flask equipped with reflux condenser and dropping funnel. A solution of 4-benzylcarbamoyl-butyric acid methyl ester **1c** (5.0 g, 18 mmol) in toluene (~30 mL) was added and mixture was refluxed for 3 h. After cooling at room temperature the mixture was filtered and the filtrate was evaporated under reduced pressure to give 65 % of compound **1** (C₁₂H₁₃NO₂). ¹H NMR (200 MHz, CDCl₃): δ = 7.36–7.24 (m, 5H, Ar-H), 4.94 (s, 2H, CH₂), 2.65 (t, *J* = 6.5 Hz, 4H, CH₂), 1.98–1.88 (m, 2H, CH₂) ppm; ¹³C NMR (50 MHz, CDCl₃): δ = 172.5 (CCO_{imide}), [137.3, 128.8, 128.4, 127.4 (C_{Ar}), 42.6 (CCH₂), 32.9 (CCH₂), 17.0 (CCH) ppm; HR-MS (ESI, *m/z*): calcd. for C₁₂H₁₃NO₂ [*M* + NH₄]⁺: 221.1284; found: 221.1278.

8-Benzyl-8-aza-spiro[4.5]decane-7,9-dione (**2**, C₁₆H₁₉NO₂). Prepared from methyl ester **2e**. Yield 75%; ¹H NMR (200 MHz, CDCl₃): δ = 7.37–7.24 (m, 5H, Ar-H), 4.94 (s, 2H, CH₂), 2.60 (s, 4H, CH₂), 1.72–1.65 (m, 4H, CH₂), 1.50–1.44 (m, 4H, CH₂) ppm; ¹³C NMR (50 MHz, CDCl₃): δ = 172.1 (CCO_{imide}), [137.2,

128.5, 128.3, 127.3 (C_{Ar}), 44.7 (CCH₂), 42.6 (CCH₂), 39.4 (C), 37.4 (CCH₂), 24.1 (CCH₂) ppm; HR-MS (ESI, *m/z*): calcd. for C₁₆H₁₉NO₂ [M + H]⁺: 258.1489; found: 258.1480.

General procedure described in our previous paper was used for preparation of compounds 3–9

2,6-Dioxo-1-phenethylpiperidine-3-carbonitrile (3, C₁₄H₁₄N₂O₂). Yield 65%; ¹H NMR (200 MHz, CDCl₃): δ = 7.34–7.19 (m, 5H, Ar–H), 4.05 (splitted t, *J* = 7.0 Hz; *J* = 2.1 Hz, 2H, CH₂), 3.71 (dd, *J* = 9.3 Hz, *J* = 5.3 Hz, 1H, CH), 2.95–2.81 (m, 3H, CH₂), 2.72–2.56 (m, 1H, CH₂), 2.36–2.17 (m, 2H, CH₂) ppm; ¹³C NMR (50 MHz, CDCl₃): δ = 169.6 (CCO_{imide}), [137.7, 129.0, 128.5, 126.7 (C_{Ar})], 115.1 (CCN), 41.6 (CCH₂), 35.7 (CCH₂), 33.6 (CCH), 30.7 (CCH₂), 21.5 (CCH₂) ppm; HR-MS (ESI, *m/z*): calcd. for C₁₄H₁₄N₂O₂ [M + NH₄]⁺: 260.1393, found: 260.1389.³⁰

Tert-pentyl-2,6-dioxo-1-phenethylpiperidine-3-carboxylate (4, C₁₉H₂₅NO₄). Yield 70%; ¹H NMR (200 MHz, CDCl₃) δ = 7.30–7.21 (m, 5H, Ar–H), 4.04–3.96 (m, 2H, CH₂), 3.57–3.51 (m, 1H, CH), 2.86–2.78 (m, 2H, CH₂), 2.67 (dt, *J* = 11.6 Hz, *J* = 5.8 Hz, 2H, CH₂), 2.25–2.07 (m, 2H, CH₂), 1.80 (q, *J* = 7.5 Hz, 2H, CH₂), 1.46 (s, 6H, CH₃), 0.90 (t, *J* = 7.5 Hz, 3H, CH₃) ppm; ¹³C NMR (50 MHz, CDCl₃): δ = 171.3 (CCO_{imide}), 168.8 (CCO_{imide}), 167.7 (CCO_{ester}), [138.4, 128.9, 126.4 (C_{Ar})], 85.6 (C), 50.0 (CCH), 41.1 (CCH₂), 33.8 (CCH₂), 33.3 (CCH₂), 30.8 (CCH₂), 30.2 (CCH₂), 25.3 (CCH₃), 20.7 (CCH₂), 8.1 (CCH₃) ppm; HR-MS (ESI, *m/z*): calcd. for C₁₉H₂₅NO₄ [M + H]⁺: 332.1856, found: 332.1841.

Tert-pentyl-1-benzyl-4-methyl-2,6-dioxopiperidine-3-carboxylate (5, C₁₉H₂₅NO₄). Yield 46.6%; ¹H NMR (200 MHz, CDCl₃): δ = 7.38–7.24 (m, 5H, Ar–H), 5.04–4.88 (m, 2H, CH₂), 3.59 (d, *J* = 4.9 Hz, 0.13 H, CH), 3.21 (d, *J* = 9.0 Hz, 0.59 H, CH), 2.83 (dd, *J* = 16.5, *J* = 3.9 Hz, 1 H, CH), 2.74–2.68 (m, 0.41 H, CH₂), 2.60–2.46 (m, 1H, CH₂), 2.43–2.29 (m, 1H, CH₂), 1.76 (dt, *J* = 9.4 Hz, *J* = 4.8 Hz, 2H, CH₂), 1.44 (s, 5H, CH₃), 1.36 (d, *J* = 3.5 Hz, 1H, CH₃), 1.14–1.07 (m, 3H, CH₃), 0.91–0.75 (m, 3H, CH₃) ppm; ¹³C NMR (50 MHz, CDCl₃): δ = 170.9 (CCO_{imide}), 169.1 (CCO_{imide}), 167.4 (CCO_{ester}), [136.9, 128.7, 128.4, 127.5 (C_{Ar})], 85.4 (C), 57.9 (CCH), 43.0 (CCH₂), 38.6 (CCH₂), 33.4 (CCH₂), 27.7 (CCH), 25.3 (CCH₃), 25.2 (CCH₂), 19.1 (CCH₃), 8.1 (CCH₃) ppm; HR-MS (ESI, *m/z*): calcd. for C₁₉H₂₅NO₄ [M + NH₄]⁺: 349.2122, found: 349.2128.

1-(*R*)-1-Phenylethyl-3-(phenylsulfonyl)piperidine-2,6-dione (6, C₁₉H₁₉NO₄S). Yield 68%; ¹H NMR (200 MHz, CDCl₃): δ = 7.90–7.26 (m, 10H, Ar–H), 6.19–6.00 (m, 1H, CH), 4.13–3.942 (m, 1H, CH), 3.44–3.14 (m, 1H, CH₂), 2.92–2.71 (m, 2H, CH₂), 2.45–2.25 (m, 1H, CH₂), 1.77–1.71 (m, 3H, CH₃) ppm; ¹³C NMR (50 MHz, CDCl₃): δ = 171.1 (CCO_{imide}), 170.8 (CCO_{imide}), [139.6, 134.5, 134.4, 129.2, 129.0, 128.1, 128.0, 127.7, 127.0, 126.8 (C_{Ar})], 66.2 (CCH), 50.3 (CCH), 50.1 (CCH), 29.8 (CCH₂), 29.4 (CCH₂), 17.6 (CCH₃), 17.4, (CCH₃), 15.8 (CCH₂) ppm; HR-MS (ESI, *m/z*): calcd. for C₁₉H₁₉NO₄S [M + H]⁺: 358.1099, found: 358.1108.

2-Benzyl-2-azaspiro[5.11]heptadecane-1,3,7-trione (7, C₂₃H₃₁NO₃). Yield 42.1%; ¹H NMR (500 MHz, CDCl₃): δ = 7.34–7.23 (m, 5H, Ar–H), 4.95 (AB_q, 2H, CH₂, *J* = 14.6 Hz), 3.23–3.17 (ddd, 1H, CH₂, *J* = 7.6 Hz, *J* = 5.3 Hz, *J* = 1.0 Hz), 2.68–2.56 (m, 2H, CH₂), 2.59–2.53 (m, 2H, CH₂), 2.00–1.95 (m, 1H, CH₂), 1.60–1.47 (m, 4H, CH₂), 1.33–1.19 (m, 15H, CH₂), 0.96–0.89 (m, 1H, CH₂) ppm; ¹³C NMR (125 MHz, CDCl₃): δ = 204.8 (CCO_{keto}), 172.7 (CCO_{imide}), 171.9 (CCO_{imide}), [136.9, 128.8, 128.4, 127.5 (C_{Ar})], 60.0 (CCH), 43.4 (CCH₂), 34.7 (CCH₂), 33.9 (CCH₂), 29.9 (CCH₂), 26.3 (CCH₂), 26.2 (CCH₂), 23.3 (CCH₂), 23.1 (CCH₂), 22.0 (CCH₂), 21.7 (CCH₂), 18.8 (CCH₂) ppm; HR-MS (ESI, *m/z*): calcd. for C₂₃H₃₁NO₃ [M + H]⁺: 370.2377, found: 370.2371.

2-Benzyl-2-azaspiro[5.7]tridecane-1,3,7-trione (8, C₁₉H₂₃NO₃). Yield 53%; ¹H NMR (200 MHz, CDCl₃): δ = 7.28–7.23 (m, 5H, Ar–H), 4.91 (s, 2H, CH₂), 3.19–2.40 (m, 6H, CH₂), 2.25 (ddd, *J* = 12.3 Hz, *J* = 6.2 Hz, *J* = 3.4 Hz, 1H, CH₂), 1.88–1.53 (m, 9H, CH₂) ppm; ¹³C NMR (50 MHz, CDCl₃): δ = 213.3 (CCO_{keto}), 172.3 (CCO_{imide}), 171.6 (CCO_{imide}), [137.0, 128.4, 128.2, 127.3 (C_{Ar})], 57.9 (C), 43.1 (CCH₂), 38.3 (CCH₂), 31.4 (CCH₂), 30.0 (CCH₂), 29.5 (CCH₂), 25.7 (CCH₂), 23.9 (CCH₂), 23.8 (CCH₂), 22.5 (CCH₂) ppm; HR-MS (ESI, *m/z*): calcd. for C₁₉H₂₃NO₃ [M + H]⁺: 314.1751, found: 314.1738.

Ethyl 4-(1-benzyl-2,6-dioxopiperidin-3-yl)butanoate (9, C₁₈H₂₃NO₄). Yield 42%; ¹H NMR (200 MHz, CDCl₃): δ = 7.37–7.22 (m, 5H, Ar–H), 4.94 (s, 2H, CH₂), 4.13 (q, *J* = 7.1 Hz, 2H, CH₂), 2.82 (dt, *J* = 17.6 Hz, *J* = 4.9 Hz, 1H, CH₂), 2.64 (dd, *J* = 11.1 Hz, *J* = 5.3 Hz, 1H, CH₂), 2.54–2.42 (m, 1H, CH), 2.34 (t, *J* = 7.2 Hz, 2H, CH₂), 2.12–1.90 (m, 2H, CH₂), 1.82–1.56 (m, 4H, CH₂), 1.25 (t, *J* = 7.1 Hz, 3H, CH₃) ppm; ¹³C NMR (50 MHz, CDCl₃): δ = 174.5 (CCO_{imide}), 173.2 (CCO_{ester}), 172.2 (CCO_{imide}), [137.3, 128.5, 128.3, 127.3 (C_{Ar})], 60.3 (CCH₂), 42.9 (CCH₂), 41.9 (CCH₂), 33.9 (CCH₂), 31.9 (CCH₂), 29.6 (CCH₂), 22.2 (CCH₂), 22.0 (CCH₂), 14.1 (CCH₃) ppm; HR-MS (ESI, *m/z*): calcd. for C₁₈H₂₃NO₄ [M + H]⁺: 318.1700, found: 318.1691.

8-Oxaspiro[4.5]decane-7,9-dione (2c) was prepared according to a modified literature procedure⁴⁷.

7,9-Dioxo-8-azaspiro[4.5]decane-6,10-dicarbonitrile (2a) and **2,2'-cyclopentane-1,1-diyl diacetic acid (2b)** were prepared by a known literature procedure⁴⁸. **Methyl 5-chloro-5-oxopentanoate (1b)** and **methyl [1-(2-chloro-2-oxoethyl)cyclopentyl] acetate (2d)** were prepared by a modification of a known literature procedure⁴⁹.

Methyl 5-(benzylamino)-5-oxopentanoate (1c) and **methyl 2-(1-(2-(benzylamino)-2-oxoethyl)cyclopentyl) acetate (2e)** were prepared according to a modified literature procedure⁵⁰.

Methyl 2-methylbutan-2-yl propanedioate (3b) was prepared by a literature procedure⁵¹. **Methyl 2-(phenylsulfonyl)acetate (3c)** was prepared by a literature procedure⁵².

Acrylamides (4a, 4c, 4d) and **(*E*)-*N*-benzylbut-2-enamide (4b)** were prepared according to a modified literature procedure⁵⁰.

β-Ketoesters (5a–c) were prepared by a modification of a literature procedure⁵³.

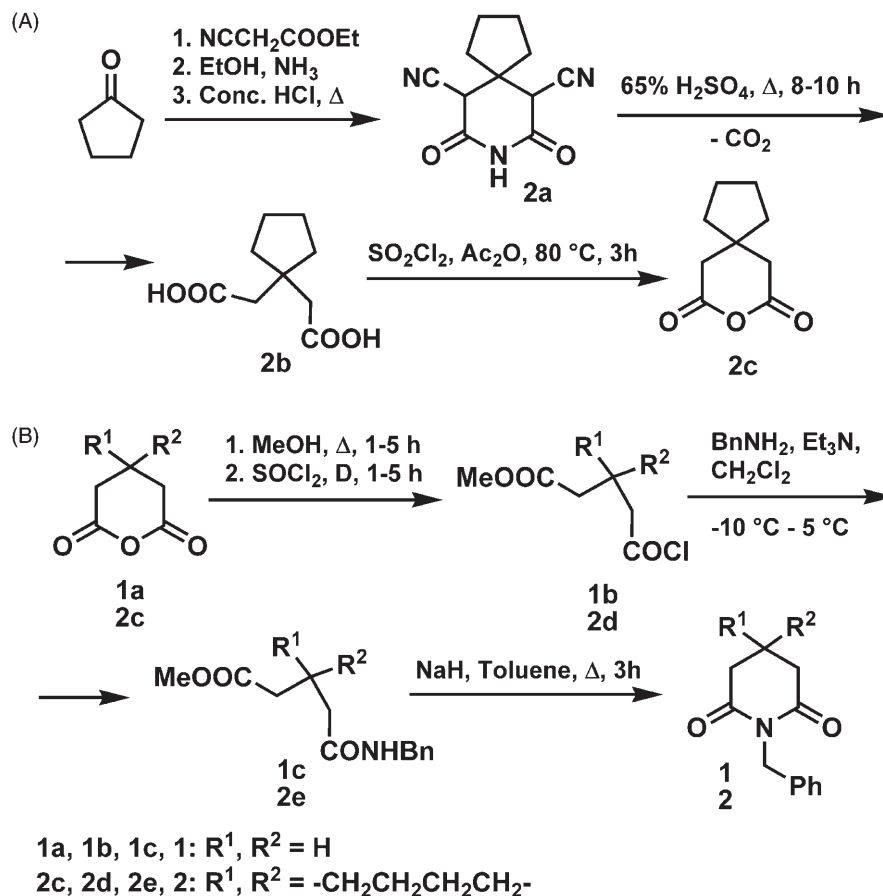
Results and discussion

Chemistry

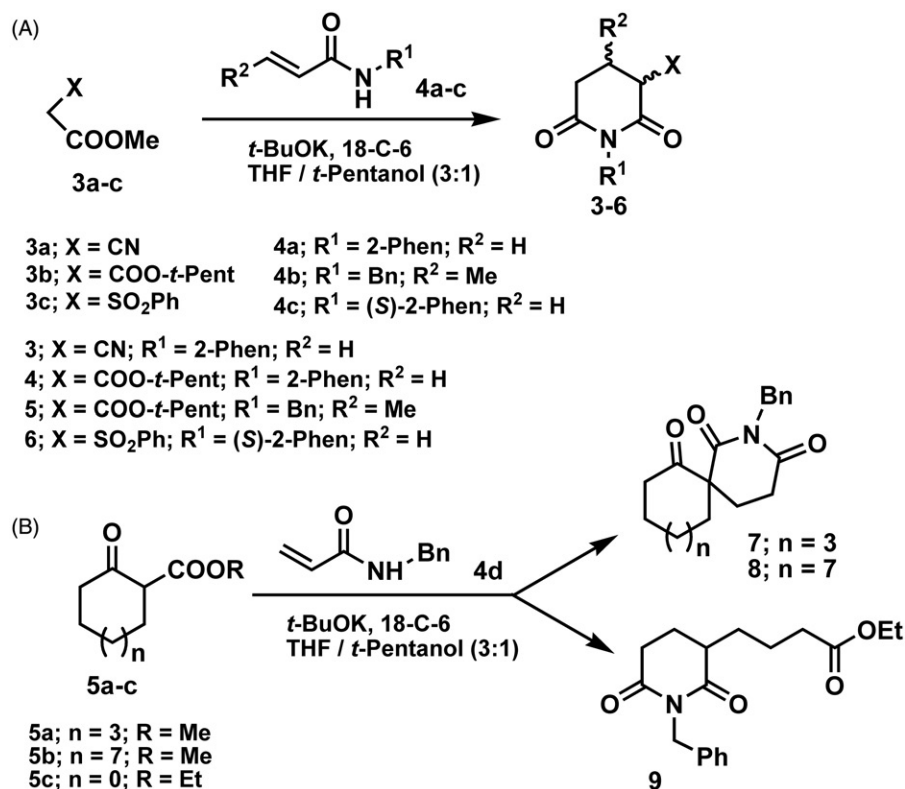
Glutarimide derivatives, depicted in Figure 1, were synthesized according to previously reported procedures of our³⁰ or other research groups. Compounds **1** and **2** were prepared according to a modified literature procedure. Cyclization of amido-esters, derived from corresponding glutaric acid anhydrides, in presence of the base (NaH), was carried out by reflux in toluene (~3 h), yielding glutarimides **1** and **2** (Scheme 1). Amido-esters **1c** and **2e** were prepared from **1a** and **2c**, respectively, by a modification of standard methods^{47,49,50}.

Compounds **3–9** were synthesized by tandem process described in our previous paper³⁰. The process involved a base-catalyzed Michael addition of active methylene compounds to secondary acrylamides or crotonamides, followed by intramolecular *N*-acylation of the carboxamido group. Synthesis of derivatives **3–6** was performed by reacting methyl 1,2-cyanoacetate (**3a**), methyl *t*-pentyl malonate (**3b**) and methyl 2-(phenylsulfonyl)acetate (**3c**) with *N*-substituted acryl- and crotonamides (**4a–c**), under the reaction conditions (Scheme 2A). Yields of products were 42–72%. In the reaction of β-keto esters, comprising **5, 8** and **12** member rings, **5a–c**, with *N*-benzyl acrylamide, imides **9, 8** and **7**, respectively, were obtained (Scheme 2B).

Scheme 1. Synthetic path to obtain compounds 1 and 2.



Scheme 2. Synthetic paths to obtain compounds (A) 3–6; and (B) 7–9.



Antiproliferative activity

The cytotoxicity of compounds **1–9** was tested toward selected human cancer cell lines: cervix adenocarcinoma HeLa, human myelogenous leukemia K562 and human breast carcinoma MDA-MB-453 cells. Cell survival was determined by MTT test, after

Table 1. Concentrations of compounds **1–9** that induced 50% decrease in cell survival (IC₅₀).

Compound	IC ₅₀ (μM)			
	HeLa	K562	MDA-MB-453	MRC5
1	>200	>200	>200	–
2	150.2 ± 2.0	103.9 ± 4.4	167.8 ± 3.8	–
3	>200	>200	>200	–
4	119.3 ± 1.3	96.6 ± 2.5	150.9 ± 0.2	–
5	108.4 ± 8.1	81.1 ± 0.8	135.7 ± 0.2	–
6	154.3 ± 6.9	147.1 ± 8.7	~200	–
7	26.8 ± 4.7	8.98 ± 0.64	27.36 ± 0.20	36.73 ± 0.65
8	146.7 ± 5.9	150.0 ± 0.1	138.1 ± 3.5	–
9	186.5 ± 1.2	193.6 ± 6.4	195.2 ± 4.8	–

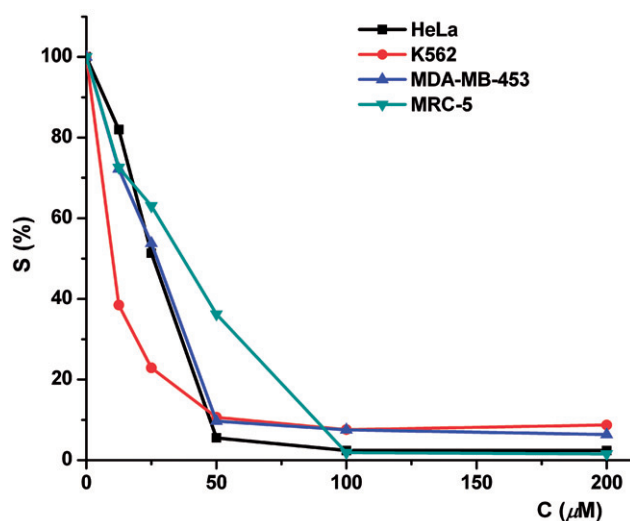


Figure 2. Dose–response curves for the cytotoxicity of compound **7** toward HeLa, K562, MDA-MB-453 and MRC-5 cells. Percentage of viable cells (S%) was plotted against various concentrations of compound **7**.

72 h of exposure to compounds^{31,32}. IC₅₀ values (Table 1) are shown in molar concentrations, as the mean ± SD, determined from three independent measurements.

IC₅₀ was defined as the concentration of the compound inhibiting cell survival by 50%, compared with a vehicle-treated control cells. The most potent compound, **7**, was also tested toward MRC-5, normal lung fibroblast cells. Compounds **2**, **4**, **5–8** and **9** exerted dose-dependent cytotoxicity toward malignant cells, while compound **7** appeared as the most active. Compound **7** exerted humble selectivity, with IC₅₀ toward normal cells ~37 μM. The decrease in survival of target cells induced by compound **7** is shown in Figure 2.

Antibacterial activity

Antibacterial activity of compounds **1**, **2**, **4–8** and **9** was examined against selected foodborne pathogenic bacteria, Gram-positive species *S. aureus* (ATCC 25923), *E. faecalis* (ATCC 29212), *B. cereus* (ATCC 10876), *L. monocytogenes* (ATCC 19115) and Gram-negative species *P. aeruginosa* (ATCC 27853), *E. coli* (ATCC 25922), *S. enteritidis* (ATCC 13076), *P. hauseri* (ATCC 13315), *S. sonnei* (ATCC 29930), *Y. enterocolitica* (ATCC 27729), *E. coli* O157:H7 (ATCC 12900). A preliminary screening, done by a disc diffusion method, indicated the ability of bacteria to produce visible growth in the presence of compounds **1**, **2**, **4–8** and **9**. In most cases, Gram-negative bacteria were more resistant to the tested compounds than Gram-positive bacteria (Table 2). The diameters of the inhibition zones, determined by a disk diffusion method, ranged from 6.4 to 14.6 mm, in the presence of 200 μg of compounds tested.

The Gram-positive bacteria *B. cereus* were the most sensitive to compounds **4** and **9** (14.6 and 14.2 mm, respectively). Such activity was comparable to the effect of commercial antibiotic gentamicin (14.8 mm). Also, there was no statistically significant difference between the susceptibility of *B. cereus* on commercial antibiotic tetracycline (12.4 mm) and compounds **2**, **7** and **8** (12.1, 12.9 and 12.4 mm, respectively). Among Gram-negative bacteria, *S. sonnei* was the most sensitive to compounds **2**, **4** and **6** (11.5, 10.4 and 10.2 mm, respectively), comparable to antibiotic tetracycline (11.4 mm). Other compounds did not show significant antimicrobial activity against tested bacteria in the applied concentration. Compound **5** did not show any antimicrobial effect on tested Gram-positive and Gram-negative bacteria.

Due to the fact that the disk diffusion method is not entirely reliable in determining the antimicrobial properties, the broth microdilution method, as a rapid and quantitative method

Table 2. Antibacterial activity of compounds **1**, **2**, **4**, **6–8** and **9**, determined by the disk diffusion method.

Bacterial strain	Diameter of inhibition zone (mm) including the initial diameter of the disk (6 mm)*								G†	T‡
	1	2	4	6	7	8	9			
<i>S. aureus</i>	8.2 ± 0.2 ^f	11.3 ± 0.4 ^d	13.3 ± 0.4 ^c	8.5 ± 0.2 ^f	12.6 ± 0.2 ^c	12.9 ± 0.1 ^c	9.8 ± 0.2 ^{e¶}	18.2 ± 0.8 ^b	29.9 ± 0.3 ^a	
<i>E. faecalis</i>	10.1 ± 0.5 ^c	10.8 ± 0.2 ^c	9.3 ± 0.2 ^d	8.1 ± 0.3 ^e	9.4 ± 0.5 ^d	10.2 ± 0.4 ^c	10.3 ± 0.2 ^c	12.1 ± 0.7 ^b	15.8 ± 0.5 ^a	
<i>B. cereus</i>	9.3 ± 0.0 ^c	12.1 ± 0.9 ^b	14.6 ± 0.3 ^a	9.6 ± 0.5 ^c	12.9 ± 0.0 ^b	12.4 ± 0.2 ^b	14.2 ± 0.1 ^a	14.8 ± 0.2 ^a	12.4 ± 0.3 ^b	
<i>L. monocytogenes</i>	9.2 ± 0.3 ^c	12.1 ± 0.2 ^b	8.3 ± 0.5 ^f	8.1 ± 0.1 ^f	10.1 ± 0.7 ^d	10.5 ± 0.5 ^d	11.6 ± 0.4 ^c	12.6 ± 0.7 ^b	15.2 ± 0.4 ^a	
<i>P. aeruginosa</i>	–§	9.6 ± 0.4 ^b	7.3 ± 0.3 ^c	7.4 ± 0.4 ^c	7.1 ± 0.3 ^c	7.0 ± 0.2 ^c	7.5 ± 0.5 ^c	21.3 ± 0.4 ^a	9.1 ± 0.2 ^b	
<i>E. coli</i>	8.3 ± 0.5 ^c	–	8.2 ± 0.5 ^c	8.0 ± 0.6 ^c	–	7.7 ± 0.1 ^c	7.9 ± 0.3 ^c	22.9 ± 0.8 ^a	11.4 ± 0.4 ^b	
<i>S. enteritidis</i>	7.9 ± 0.3 ^d	8.3 ± 0.6 ^d	9.1 ± 0.1 ^c	7.1 ± 0.2 ^e	–	–	6.8 ± 0.6 ^e	25.3 ± 0.4 ^a	22.5 ± 0.6 ^b	
<i>P. hauseri</i>	–	–	6.9 ± 0.3 ^d	8.6 ± 0.6 ^c	6.4 ± 0.7 ^d	6.8 ± 0.3 ^d	–	25.6 ± 0.5 ^a	24.8 ± 0.3 ^b	
<i>S. sonnei</i>	9.7 ± 0.6 ^d	11.5 ± 0.8 ^b	10.4 ± 0.3 ^c	10.2 ± 0.2 ^c	9.8 ± 0.1 ^d	9.9 ± 0.4 ^d	8.7 ± 0.0 ^c	16.6 ± 0.4 ^a	11.4 ± 0.4 ^b	
<i>Y. enterocolitica</i>	8.9 ± 0.0 ^c	8.4 ± 0.6 ^c	8.6 ± 0.2 ^c	7.4 ± 0.3 ^d	7.7 ± 0.2 ^d	7.9 ± 0.3 ^d	7.1 ± 0.4 ^d	30.9 ± 0.4 ^a	26.8 ± 0.8 ^b	
<i>E. coli</i> (O157:H7)	8.1 ± 0.7 ^c	–	7.6 ± 0.3 ^c	7.8 ± 0.1 ^c	–	–	–	21.8 ± 0.6 ^b	33.7 ± 0.1 ^a	

*Data are expressed as mean ± standard deviation (n = 3).

†G-gentamicin.

‡T-tetracycline.

¶Within the same row, means followed by different letters are significantly different at p < 0.05 (ANOVA, Fisher's LSD).

§Inhibition zone not achieved.

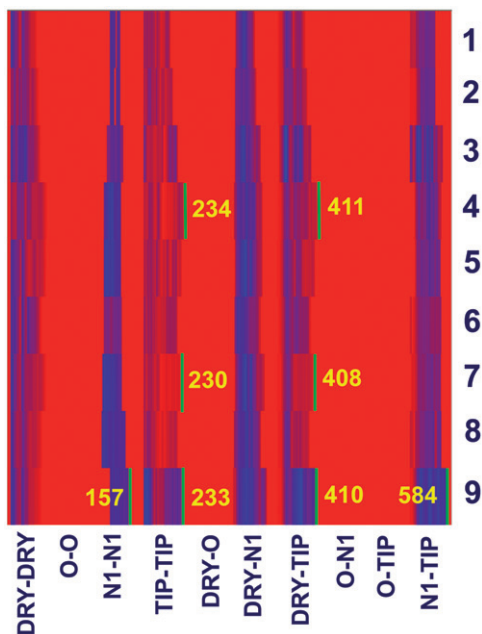


Figure 3. Heatmap depiction of descriptors (auto- and cross-correlograms), calculated by AMANDA algorithm, for compounds 1–9.

for determining of MIC, based on the color change caused by the enzymatic activity of viable microorganisms, was applied (Table 3). Compounds 1, 2, 4, 6–8 and 9 inhibited the growth of all tested Gram-positive and some of the Gram-negative bacteria. Achieved MICs were in the range of $0.625\text{--}10.0\text{ mg/mL}$ ($1.97 \times 10^{-3}\text{--}4.92 \times 10^{-2}\text{ mol/L}$).

The highest antibacterial potential was reached with compound 9 against *B. cereus* (MIC was $0.625\text{ mg/mL} = 1.97 \times 10^{-3}\text{ mol/L}$). MICs against Gram-negative bacteria exceeded 10.0 mg/mL , for the majority of compounds, including compound 5, proved to be inactive in concentrations up to 10.0 mg/mL against all bacterial strains tested. Exceptions were compound 4, whose antibacterial activity ranged from 5.0 to 10.0 mg/mL against all tested Gram-negative bacteria and compounds 2, 6 and 7, with MICs of 10.0 mg/mL (3.89×10^{-2} , 2.80×10^{-2} and $2.71 \times 10^{-2}\text{ mol/L}$, respectively) against *S. sonnei*.

Structure–activity relationship

Although exerting humble potency, derivatives 9 and 4 appeared most potent against bacteria, while derivative 7 was the one with fair potency toward human tumor cells. In order to rationalize structural features associated with the most potent compounds we calculated molecular descriptors derived from the 3D structures of compounds. For modeling studies structures of all compounds (1–9) were prepared as described in our previous paper⁵⁴, see section ‘‘Methods’’. Due to low number of compounds tested against bacteria, or toward human tumor cells, and limited potencies, we did not build novel quantitative structure–activity models, but envisaged to use molecular properties and to use previously built model to draw conclusions on structural characteristics needed for significant potency. To predict potency of compound 7 toward K562 cells, we projected structures of compounds 2, 7 and 8 (all spirocyclic compounds in our dataset) on model previously derived for antiproliferative activity data of glutarimide derivatives toward K562 cells, collected from National Cancer Institute (NCI) repository⁵⁴. Unfortunately, our prediction failed. Compounds 2 and 7 were predicted as more potent comparing to compound 8 (data not shown). There are several possible reasons for the poor prediction. First, in the

Table 3. Antibacterial activity of compounds 1, 2, 4, 6–8 and 9 expressed as MIC (mg/mL), determined by the broth microdilution method.

Bacterial strain	MIC (mg/mL)*												
	1	2	4	6	7	8	9						
<i>S. aureus</i>	5.0 ± 0.0^b	2.46×10^{-2}	5.0 ± 0.0^b	1.94×10^{-2}	2.5 ± 0.0^c	7.54×10^{-3}	5.0 ± 0.0^b	1.40×10^{-2}	2.71×10^{-2}	10.0 ± 0.0^d	3.19×10^{-2}	$5.0 \pm 0.0^{b\dagger}$	1.58×10^{-2}
<i>E. faecalis</i>	10.0 ± 0.0^a	4.92×10^{-2}	5.0 ± 0.0^b	1.94×10^{-2}	2.5 ± 0.0^c	7.54×10^{-3}	5.0 ± 0.0^b	1.40×10^{-2}	1.35×10^{-2}	5.0 ± 0.0^b	1.59×10^{-2}	5.0 ± 0.0^b	1.58×10^{-2}
<i>B. cereus</i>	5.0 ± 0.0^a	2.46×10^{-2}	1.25 ± 0.0^b	4.90×10^{-3}	1.25 ± 0.0^b	3.77×10^{-3}	5.0 ± 0.0^a	1.40×10^{-2}	3.40×10^{-3}	1.25 ± 0.0^b	4.00×10^{-3}	0.625 ± 0.0^c	1.97×10^{-3}
<i>L. monocytogene</i>	10.0 ± 0.0^a	4.92×10^{-2}	2.5 ± 0.0^c	9.7×10^{-3}	10.0 ± 0.0^a	3.02×10^{-2}	10.0 ± 0.0^a	2.80×10^{-2}	1.35×10^{-2}	5.0 ± 0.0^b	1.59×10^{-2}	10.0 ± 0.0^a	3.15×10^{-2}
<i>P. aeruginosa</i>	$>10 \pm 0.0$	$>10 \pm 0.0$	10.0 ± 0.0	3.02×10^{-2}	10.0 ± 0.0	3.02×10^{-2}	$>10 \pm 0.0$	$>10.0 \pm 0.0$	$>10.0 \pm 0.0$	$>10.0 \pm 0.0$	$>10.0 \pm 0.0$	$>10.0 \pm 0.0$	$>10.0 \pm 0.0$
<i>E. coli</i>	$>10 \pm 0.0$	$>10 \pm 0.0$	10.0 ± 0.0	3.02×10^{-2}	10.0 ± 0.0	3.02×10^{-2}	$>10 \pm 0.0$	$>10.0 \pm 0.0$	$>10.0 \pm 0.0$	$>10.0 \pm 0.0$	$>10.0 \pm 0.0$	$>10.0 \pm 0.0$	$>10.0 \pm 0.0$
<i>S. enteritidis</i>	$>10 \pm 0.0$	$>10 \pm 0.0$	10.0 ± 0.0	3.02×10^{-2}	10.0 ± 0.0	3.02×10^{-2}	$>10 \pm 0.0$	$>10.0 \pm 0.0$	$>10.0 \pm 0.0$	$>10.0 \pm 0.0$	$>10.0 \pm 0.0$	$>10.0 \pm 0.0$	$>10.0 \pm 0.0$
<i>S. hauseri</i>	$>10 \pm 0.0$	$>10 \pm 0.0$	10.0 ± 0.0	3.89×10^{-2}	10.0 ± 0.0	3.02×10^{-2}	$>10 \pm 0.0$	$>10.0 \pm 0.0$	$>10.0 \pm 0.0$	$>10.0 \pm 0.0$	$>10.0 \pm 0.0$	$>10.0 \pm 0.0$	$>10.0 \pm 0.0$
<i>S. sonnei</i>	$>10 \pm 0.0$	$>10 \pm 0.0$	10.0 ± 0.0	3.89×10^{-2}	5.0 ± 0.0	1.51×10^{-2}	10.0 ± 0.0	2.80×10^{-2}	2.71×10^{-2}	10.0 ± 0.0	$>10.0 \pm 0.0$	$>10.0 \pm 0.0$	$>10.0 \pm 0.0$
<i>Y. enterocolitica</i>	$>10 \pm 0.0$	$>10 \pm 0.0$	10.0 ± 0.0	3.02×10^{-2}	10.0 ± 0.0	3.02×10^{-2}	$>10 \pm 0.0$	$>10.0 \pm 0.0$	$>10.0 \pm 0.0$	$>10.0 \pm 0.0$	$>10.0 \pm 0.0$	$>10.0 \pm 0.0$	$>10.0 \pm 0.0$
<i>E. coli</i> (O157:H7)	$>10 \pm 0.0$	$>10 \pm 0.0$	10.0 ± 0.0	3.02×10^{-2}	10.0 ± 0.0	3.02×10^{-2}	$>10 \pm 0.0$	$>10.0 \pm 0.0$	$>10.0 \pm 0.0$	$>10.0 \pm 0.0$	$>10.0 \pm 0.0$	$>10.0 \pm 0.0$	$>10.0 \pm 0.0$

*Data are expressed as mean \pm standard deviation ($n = 3$).

†Within the same row, means followed by different letters are significantly different at $p < 0.05$ (ANOVA, Fisher's LSD).

model of antiproliferative activity of NCI glutarimides toward K562 cells, potency data span range from 4 to 8.6 ($p(GI_{50})$ values). Approximating equality between $p(IC_{50})$ and $p(GI_{50})$ values, which for sure is not the most stringent criteria; compounds **2** and **7**, with $p(IC_{50})$ of 3.98 and 3.82, respectively, are out of the range of potencies that NCI model covers. Next, antiproliferative data of compounds tested by NCI were obtained by Sulforhodamine B assay after 48 h of exposure of cells to compounds, while we used MTT assay and exposed cells to compounds during 72 h. The most potent compounds in NCI set comprise unsubstituted glutarimide nitrogen, while all compounds in our set bear bulky substituent in this position. Finally, our model of antiproliferative activity of NCI glutarimides was built on the pharmacophoric similarity patterns (including spatial positions of HBA, HBD, hydrophobic and shape features), but did not include whole-molecule properties, as surfaces and volumes. Next, we compared whole-molecular properties of compounds **1–9** (surface area, polar surface area, apolar surface area, volume, virtual log *P*; Supplemental Information, Table S1) derived from the 3D structures of compounds. We concluded that derivative **7**, most potent toward human tumor cells tested, had the largest molecular volume. This observation is in accordance with the fact that compounds having largest molecular volumes are among most potent in NCI glutarimide set (Figure 4a in reference⁵⁴). To obtain more data on structural features associated with most potent compounds in our set, we calculated MIF, with hydrogen-bond donor (N1), hydrogen-bond acceptor (O), hydrophobic (DRY) and shape (TIP) probes around compounds **1–9** in program Pentacle, and visually inspected interaction patterns, obtained by two-point pharmacophoric features offered by AMANDA algorithm^{45,55}. Blocks of correlograms were depicted as a heatmap (Figure 3). Features that separate the most potent compounds from the rest appeared straightforwardly.

We observed TIP-TIP and DRY-TIP blocks of variables which were broader for compounds **4**, **7** and **9**, comparing with the same block of variables for the rest of compounds. Along with this, the N1-TIP block of variables is significantly broader for compound **9**, compared to other compounds. So, variables in those three blocks, with the largest distances between nodes, made distinction between compounds **4**, **7** and **9** and the rest. Variables TIP-TIP-230, encoding nodes of shape probe on distance of ~ 17.1 Å (Supplemental Information, Figure S19a), and DRY-TIP-408, encoding node of hydrophobic probe and the node of shape probe on distance of ~ 17.4 Å (Supplemental Information, Figure S19b), clearly separated compound **7**, most potent toward tumor cells tested, from the rest. Along the largest molecular volume, compound **7** comprises bulky cycloalkyl moiety distal from the benzyl ring bound to glutarimide N. We observed similar structural features for compounds **9** and **4**, most active against Gram-positive bacteria. Variables TIP-TIP-233 (nodes of the shape probe on distance of ~ 18.1 Å) and DRY-TIP-410 (node of the hydrophobic probe on distance of ~ 18.1 Å from the node of shape probe) encoded compound **9**. Variables TIP-TIP-234 (nodes of the shape probe on distance of ~ 18.4 Å) and DRY-TIP-411 (node of the hydrophobic probe on distance of ~ 18.4 Å from the node of shape probe) encode compound **4**. Along with those two variables, comparable with variables associated with compound **7**, that described overall shape and spatial position of benzyl moiety and branched alkyl chains attached to position 3 of glutarimide ring in compounds **9** and **4**; we observed additional variables characteristic for compound **9**. Variables N1-TIP-584 (HBD associated with keto group in glutarimide ring, and alkyl moiety of the ester, associated with the shape probe, on spatial distance of ~ 17.1 Å) and N1-N1-157 (HBDs associated with keto group in glutarimide ring and with ester keto moiety) are typical for compound **9**. We did not observe similar variables for compound

4, most probably because ester keto group, as a HBA, was hindered with branched alkyl moiety. All variables described for compounds **9** and **4** are depicted in Figures S20 and S21 (Supplemental Information). So, along with overall large molecular volumes, due to alkyl chains bound to position 3 of glutarimide moiety, compound **9**, which exerted better antibacterial activity than the rest of compounds, has HBA moiety in this alkyl chain and this HBA is not hindered by the vicinal parts of molecule.

Conclusion

The cytotoxicity study of compounds **1–9** toward selected human cancer cell lines showed that compound **7** was the most potent, with IC_{50} values 8.98, 26.8 and 27.36 μ M, toward K562, HeLa and MDA-MB-453 cells, respectively. This compound exerted modest selectivity toward normal control MRC-5 cells with $IC_{50} \sim 37$ μ M. Preliminary screening of antibacterial activity by a disk diffusion method showed that Gram-positive bacteria were more susceptible to tested compounds than Gram-negative bacteria. Compounds **4** and **9** expressed the highest inhibition on growth of Gram-positive bacteria *B. cereus* and it is comparable to antibiotic gentamicin. *S. sonnei* (Gram-negative bacteria) was the most sensitive to the compound **2** (comparable to antibiotic tetracycline). Using a quantitative method for determination of MIC the highest antibacterial potential was achieved with compound **9** against *B. cereus*. Compound **5** did not show any antimicrobial effect on tested Gram-positive and Gram-negative bacteria in any of applied tests. Whole-molecular descriptors derived from 3D structures of examined compounds and structure–activity model based on MIF, calculated by the GRID method, rationalized structural features associated with the most potent compounds. Compound with bulky hydrophobic moiety distal from glutarimide ring exerted best antiproliferative potency within studied set.

We found that compound **7** exerts the highest antiproliferative potency within studied set. This derivative will be a starting point for further structural modifications in order to obtain more potent compounds. As compound **7** exerts modest selectivity, the second goal of structural modifications will be improvement of selectivity of new derivatives.

Declaration of interest

The authors have no conflicts of interest. Authors acknowledge the Ministry of Education, Science and Technological Development of the Republic of Serbia for financial support (Grant Nos. 172032 and 175011).

References

- Matsuda F, Terashima S. Total synthesis of natural (+)-sesbanimide A and (–)-sesbanimide B. *Tetrahedron* 1988;44:4721–36.
- Ju J, Rajski SR, Lim SK, et al. Lactimidomycin iso-migrastatin and related glutarimide-containing 12-membered macrolides are extremely potent inhibitors of cell migration. *J Am Chem Soc* 2009;131:1370–1.
- Schneider-Poetsch T, Ju J, Eyler DE, et al. Inhibition of eukaryotic translation elongation by cycloheximide and lactimidomycin. *Nat Chem Biol* 2010;6:209–17.
- Sugawara K, Nishiyama Y, Toda S, et al. Lactimidomycin, a new glutarimide group antibiotic. Production, isolation, structure and biological activity. *J Antibiot* 1992;45:1433–41.
- Machado AL, Lima LM, Araujo Jr JX, et al. Design, synthesis and antiinflammatory activity of novel phthalimide derivatives, structurally related to thalidomide. *Bioorg Med Chem Lett* 2005;15:1169–72.
- Bartlett JB, Dredge K, Dagleish AG. The evolution of thalidomide and its IMiD derivatives as anticancer agents. *Nat Rev Cancer* 2004;4:314–22.

7. Wu YH, Rayburn JW, Allen LE, et al. Psychoedative agents. 2. 8-(4-Substituted 1-piperazinylalkyl)-8-azaspiro[4.5]decane-7,9-diones. *J Med Chem* 1972;15:477–9.
8. Barrdell LB, Fitton A. Tandospirone. *CNS Drugs* 1996;5:147–52.
9. Obrig TG, Culp WJ, McKeenan WL, Hardesty B. The mechanism by which cycloheximide and related glutarimide antibiotics inhibit peptide synthesis on reticulocyte ribosomes. *J Biol Chem* 1971;246:174–81.
10. Kondo H, Oritani T, Kiyota H. Synthesis and antifungal activity of the four stereoisomers of streptimidone, a glutarimide antibiotic from *Streptomyces rimosus* forma *paromomycinus*. *Eur J Org Chem* 2000;2000:3459–62.
11. Frohardt RP, Dion HW, Jakubowski ZL, et al. Chemistry of streptimidone, a new antibiotic. *J Am Chem Soc* 1959;81:5500–6.
12. Kim BS, Moon SS, Hwang BK. Isolation, antifungal activity, and structure elucidation of the glutarimide antibiotic, streptimidone, produced by *Micromonospora coerulea*. *J Agric Food Chem* 1999;47:3372–80.
13. Ha DKK, Lau WH. Effect of recombinant human tumor necrosis factor on human nasopharyngeal carcinoma cell line *in vitro*. *Cancer Lett* 1988;41:217–24.
14. Andres MI, Sanz P, Garfia A, et al. Induction of cell differentiation and other *in vitro* effects of cycloheximide on neuroblastoma cells. *In Vitro Mol Toxicol* 1977;10:319–28.
15. Ishikawa Y, Tachibana M, Matsui C, et al. Synthesis and biological evaluation on novel analogs of 9-methylstreptimidone, an inhibitor of NF- κ B. *Bioorg Med Chem Lett* 2009;19:1726–8.
16. Powell RG, Smith Jr CR, Weisleder D. Sesbanimide A and related tumor inhibitors from *Sesbania drummondii*: structure and chemistry. *Phytochemistry* 1984;23:2789–96.
17. Powell RG, Smith CR, Weisleder D, et al. Sesbanimide, a potent antitumor substance from *Sesbania drummondii* seed. *J Am Chem Soc* 1983;105:3739–41.
18. Powel RG, Smith Jr CR. An investigation of the antitumor activity of *Sesbania drummondii*. *J Nat Prod* 1981;44:86–90.
19. Powel RG, Smith Jr CR, Madrigal RV. Antitumor activity of *Sesbania vesicaria*, *S. punicea*, and *S. drummondii* seed extracts. *Planta Med* 1976;30:1–8.
20. Armoiry X, Aulagner G, Facon T. Lenalidomide in the treatment of multiple myeloma: a review. *J Clin Pharm Ther* 2008;33:219–26.
21. Lentzsch S, Rogers MS, LeBlanc R, et al. S-3-Amino-phthalimidoglutarimide inhibits angiogenesis and growth of B-cell neoplasias in mice. *Cancer Res* 2002;62:2300–5.
22. McCarthy PL, Owzar K, Hofmeister CC, et al. Lenalidomide after stem-cell transplantation for multiple myeloma. *N Engl J Med* 2012;366:1770–81.
23. Fischer DS, Woo LW, Mahon MF, et al. D-ring modified estrone derivatives as novel potent inhibitors of steroid sulfatase. *Bioorg Med Chem* 2003;11:1685–700.
24. Brueggemeier RW, Hackett JC, Diaz-Cruz ES. Aromatase inhibitors in the treatment of breast cancer. *Endocr Rev* 2005;26:331–45.
25. Santen RJ, Brodie H, Simpson ER, et al. History of aromatase: saga of an important biological mediator and therapeutic target. *Endocr Rev* 2009;30:343–75.
26. Antonini I, Volpini R, Dal Ben D, et al. Design, synthesis, and biological evaluation of new mitonafide derivatives as potential antitumor drugs. *Bioorg Med Chem* 2008;16:8440–6.
27. Norton JT, Witschi MA, Luong L, et al. Synthesis and anticancer activities of 6-amino amonafide derivatives. *Anti-Cancer Drugs* 2008;19:23–36.
28. Wu A, Xu Y, Qian X, et al. Novel naphthalimide derivatives as potential apoptosis-inducing agents: design, synthesis and biological evaluation. *Eur J Med Chem* 2009;44:4674–80.
29. Machado KE, Navakoski de Oliveira K, Santos-Bubniak L, et al. Evaluation of apoptotic effect of cyclic imide derivatives on murine B16F10 melanoma cells. *Bioorg Med Chem* 2011;19:6285–91.
30. Popović-Đorđević JB, Ivanović MD, Kiricojević VD. A novel tandem process leading to functionalized glutarimides. *Tetrahedron Lett* 2005;46:2611–14.
31. Mosmann T. Rapid colorimetric assay for cellular growth and survival: application to proliferation and cytotoxicity assays. *J Immunol Methods* 1983;65:55–63.
32. Ohno M, Abe T. Rapid colorimetric assay for the quantification of leukemia inhibitory factor (LIF) and interleukin-6 (IL-6). *J Immunol Methods* 1991;145:199–203.
33. Tepe B, Daferera D, Sokmen A, et al. Antimicrobial and antioxidant activities of the essential oil and various extracts of *Salvia tomentosa* Miller (Lamiaceae). *Food Chem* 2005;90:333–40.
34. Clinical and Laboratory Standards Institute (CLSI). Performance standards for antimicrobial susceptibility testing: 15th informational supplement 2005. CLSI Document M100-S15. Pennsylvania: CLSI.
35. Klančnik A, Piskernik S, Jeršek B, Smole Možina S. Evaluation of diffusion and dilution methods to determine the antibacterial activity of plant extracts. *J Microbiol Methods* 2010;81:121–6.
36. Sadowski J, Gasteiger J. From atoms and bonds to three-dimensional atomic coordinates: automatic model builders. *Chem Rev* 1993;93:2567–81.
37. Sadowski J, Gasteiger J, Klebe G. Comparison of automatic three-dimensional model builders using 639 X-ray structures. *J Chem Inform Model* 1994;34:1000–8.
38. Pedretti A, Villa L, Vistoli G. VEGA – an open platform to develop chemo-bio-informatics applications, using plug-in architecture and script programming. *J Comput-Aided Mol Des* 2004;18:167–73.
39. Halgren TA. MMFF VI. MMFF94s option for energy minimization studies. *J Comput Chem* 1999;20:720–9.
40. Harrison RW. Stiffness and energy conservation in molecular dynamics: an improved integrator. *J Comput Chem* 1993;14:1112–22.
41. Stewart JJP. Optimization of parameters for semiempirical methods V: modification of NDDO approximations and application to 70 elements. *J Mol Model* 2007;13:1173–213.
42. Stewart JJP. MOPAC: a semiempirical molecular orbital program. *J Comput-Aided Mol Des* 1990;4:1–103.
43. Gaillard P, Carrupt PA, Testa B, Boudon A. Molecular lipophilicity potential, a tool in 3D QSAR: method and applications. *J Comput-Aided Mol Des* 1994;8:83–96.
44. Goodford PJ. A Computational procedure for determining energetically favorable binding sites on biologically important macromolecules. *J Med Chem* 1985;28:849–57.
45. Durán Á, Martínez GC, Pastor M. Development and validation of AMANDA, a new algorithm for selecting highly relevant regions in molecular interaction fields. *J Chem Inform Model* 2008;48:1813–23. Pentacle 1.0.6. <http://www.moldiscovery.com/software/pentacle/>
46. Gokel GW, Cram DJ, Liotta CL, et al. 18-Crown-6 (1,4,7,10,13,16-hexaoxacyclooctadecane). *Org Syn* 1988;VI:301–2.
47. Cason J. β -Methylglutaric anhydride. *Org Syn* 1963;IV:630–1.
48. Farmer HH, Rebjohn N. β -Ethyl- β -methylglutaric acid. *Org Syn* 1963;IV:441–2.
49. Cason J. β -Carbomethoxypropionyl chloride. *Org Syn* 1955;III:169–70.
50. Vogel AI. Vogel's text book of practical organic chemistry. 5th ed. Harlow: Longman Group, UK Limited; 1989.
51. Strube RE. Ethyl *tert*-butyl malonate. *Org Syn* 1963;IV:417–18.
52. Paquet LA, ed. Encyclopedia of reagents for organic synthesis. Vol. 7. Pennsylvania State University, John-Wiley; 1995. Available from: <http://eu.wiley.com/WileyCDA/WileyTitle/productCd-0470017546.html> [last accessed 21 Jul 2015].
53. Krapcho AP, Diamanti J, Cayen C, Bingham R. 2-Carboethoxycyclooctanone. *Org Syn* 1973;V:198–9.
54. Popović-Djordjević JB, Došen-Mićović LjI, Juranić IO, Drakulić BJ. Antiproliferative activity of NCI-DTP glutarimide derivatives: an alignment independent 3D QSAR study. *J Serbian Chem Soc* 2010;75:1167–79.
55. Cruciani G, ed. Methods and principles in medicinal chemistry, molecular interaction fields: applications in drug discovery and ADME prediction. Weinheim: Wiley-VCH; 2006.